

1992

## Computer Modeling: The Adjunct Micro Technique for Lipids

J. W. Hagemann

J. A. Rothfus

Follow this and additional works at: <https://digitalcommons.usu.edu/foodmicrostructure>

 Part of the [Food Science Commons](#)

---

### Recommended Citation

Hagemann, J. W. and Rothfus, J. A. (1992) "Computer Modeling: The Adjunct Micro Technique for Lipids," *Food Structure*: Vol. 11 : No. 2 , Article 1.

Available at: <https://digitalcommons.usu.edu/foodmicrostructure/vol11/iss2/1>

This Article is brought to you for free and open access by the Western Dairy Center at DigitalCommons@USU. It has been accepted for inclusion in Food Structure by an authorized administrator of DigitalCommons@USU. For more information, please contact [digitalcommons@usu.edu](mailto:digitalcommons@usu.edu).



## COMPUTER MODELING: THE ADJUNCT MICRO TECHNIQUE FOR LIPIDS

J. W. Hagemann\* and J. A. Rothfus  
U.S. Department of Agriculture, Agricultural Research Service,  
National Center for Agricultural Utilization Research  
1815 North University Street  
Peoria, Illinois 61604

### Abstract

Chemistry by computer provides access to micro-system information not readily achieved by other means. Simple computational analysis of saturated triglyceride polymorphism by molecular mechanics within constraints provided by X-ray data show that polymethylene interactions determine hydrocarbon crystal properties when they account for more than 60 percent of the total molecular interaction energy. Modeling predicts multiple, nearly equivalent,  $\alpha$ -form triglycerides and  $\alpha$ -form character in liquid near-crystalline triglycerides. Symmetrical molecules pack better than asymmetric molecules in  $\alpha$ -form configurations and transform readily to  $\beta'$ -forms if activated sufficiently to disrupt lateral chain interaction and allow dimensional displacements during transformation. The formation of  $\beta'$ -forms, thought important for quality in certain foods, may depend on controlling both the configuration of  $\alpha$ -form precursors and the sequence of molecular events during the transformation.

**Key Words:** Lipid polymorphism, molecular conformation and interaction, saturated monoacid triglycerides, subcell arrangements and symmetry, molecular energy calculations.

---

Initial paper received October 28, 1991  
Manuscript received May 6, 1992  
Direct inquiries to J.W. Hagemann  
Telephone number: 309-685-4011 ext. 235  
Fax number: 309-671-7814

---

### Introduction

Powerful tools for computer modeling and electron microscopy promise major progress toward realistic views of chemistry and biology at the molecular level. Chemists already command physical methods and computational modeling theory that provide detailed, albeit indirect, knowledge of small molecules and the ways in which they interact physically and chemically. Biologists anticipate that understanding of the operation of biological structures; e.g., cells, plastids, membranes, genes, etc., will soon be common by direct observation via various types of proximal probe analyses exemplified by scanning tunneling microscopy, STM, (Smith *et al.*, 1987; Zasadzinski *et al.*, 1988).

Combinations of computational chemistry and proximal probe analysis should allow manipulative access to intermediate levels of molecular organization that give rise to microstructure and useful chemical and biological properties. Indeed, such combinations may be the most effective way to experiment systematically with complex molecular populations.

STM allows direct recognition of atoms in planar populations of molecules and thereby delivers valuable knowledge of molecular conformation and packing, but it is limited to surface images and is susceptible to gap resistance artifacts. Computer modeling is free of such concerns, but practical limits on computation require that larger models, particularly those that involve dynamic molecules, be constrained by real data of the type collected via microscopy, X-ray diffraction, nuclear magnetic resonance (NMR), etc. Computer modeling as an extension of microscopy provides the means to evaluate images, identify artifacts, perturb organized molecular systems, analyze ultrafast transitions and easily search for novel alternatives or improved structures. This capability is especially important in studies of biomembranes and similar systems in which lipid-rich gel or liquid crystal phases may exist simultaneously.

Models facilitate analysis of complex structures and interactions. Much of contemporary molecular biology, for example, follows from insight allowed by early modeling of nucleic acid interactions. Proteins, carbohydrates, and other materials in which chemical

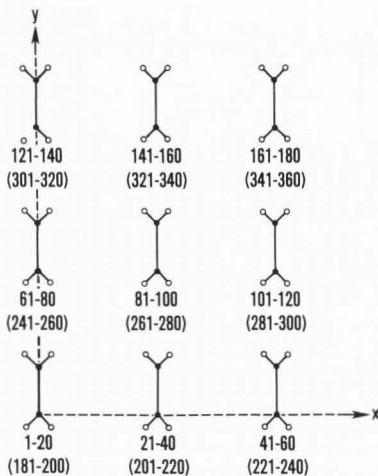


Fig. 1. Carbon atom arrangement and numbering in hydrocarbon chain segments. Solid circles indicate carbon atoms; open circles, hydrogen. Chains, represented by connected methylene groups, extend out of the plane of the figure. Numbers in parentheses refer to chains, not shown, placed over those shown; i.e., chain 261-280 is above and in line with chain 81-100 such that methyls at carbons 100 and 261 lie directly across the methyl gap. See text and Hagemann and Rothfus (1979).

structure restricts conformational freedom have yielded to computational analysis by a variety of methods (Kollman, 1987), but lipids, which are less constrained, have not been analyzed as thoroughly even though they are crucial constituents of microstructure and are relatively simple chemically.

A half-century ago, Clarkson and Malkin (1934) demonstrated that the multiple melting behavior of triglycerides involves polymorphism, in which molecular populations adopt distinct solid-phase configurations without changing covalent structure. Triglyceride conformation in the highest melting ( $\beta$ -form) configuration is known from single-crystal X-ray analyses of Larsson (1965a) refined by Gibon *et al.* (1984), but molecular conformations of low ( $\alpha$ ) and intermediate ( $\beta'$ ) melting configurations remain unknown, as do mechanisms for phase transformations and interactions with non-lipids. Given understanding of such materials and mechanisms, it should be possible to design lipid systems with specified physical properties. Combinations of microscopy and computer modeling will simplify the task.

Some of the first computer-aided modeling studies involving lipids examined gel to liquid crystal transitions

of phospholipids. For example, McAlister *et al.* (1973), applied the Lennard-Jones potential function to compute preferred conformations of non-hydrated phospholipids. Kreissler *et al.* (1983) later used statistical calculations and semi-empirical methods to demonstrate a role for water in phospholipid configurations. Computational analysis of triglycerides utilizes similar approaches, but the chemical simplicity of triglycerides leaves them more capable of molecular motion that complicates analyses of single-molecule conformation and, for practical purposes, obviates rigorous quantum mechanical approaches. Nonetheless, the distribution of triglycerides and their importance in living systems and foods justify the development of tools for predicting and regulating their behavior. Thus, de Jong and van Soest (1978) used packing analyses of double chain length conformations to develop unit cell dimensions and atomic coordinates that agreed well with X-ray diffraction data; Mattice (1979) determined the size and asymmetry of unperturbed triglycerides by calculating radii of gyration and moments of inertia; and Govil *et al.* (1978) and Hosur *et al.* (1979) identified preferred conformations of glycerol trivalerate by computing perturbative configuration interactions using localized orbitals.

A need to understand the molecular basis for thermal behavior, especially, compels triglyceride modeling. Analyses on monoacid triglycerides (Lutton and Fehl, 1970; Hagemann *et al.*, 1972; Hagemann and Rothfus, 1983a) reveal yet unexplained polymorphic behavior associated with both covalent structure and thermal treatment. The following report summarizes development of approaches to triglyceride modeling and illustrates how data from other methods of physical analysis are needed to constrain models.

### Hydrocarbon Chains

Though joined to glycerol by relatively polar ester linkages, the aliphatic chains of triglycerides enter into hydrocarbon interactions that are the source of characteristic properties. To assess the contributions of different chain arrangements, a three-dimensional array of 18 hydrocarbon chains, each chain containing 20 carbon atoms, was constructed in the computer (Hagemann and Rothfus, 1979). Nine of the chains were arranged as shown in Fig. 1, where each chain is represented by connected methylene groups. A second block of chains, not shown, was placed directly above the first group such that, for example, the methyl group at carbon 100 was directly across the methyl gap from the methyl group at carbon 261. The four subcell arrangements of hydrocarbons (Turner, 1971),  $\beta$  orthogonal,  $\beta$  monoclinic,  $\beta$  triclinic, and  $\alpha$  hexagonal, were generated by twisting carbon zigzag planes and/or by Z-direction displacements of entire chains. In these derived arrangements, carbon atoms 90-100 (Fig. 1), representing a half-chain length, were completely surrounded by other methylene or methyl groups, and were therefore suitable for computing methylene and methyl carbon interactions.

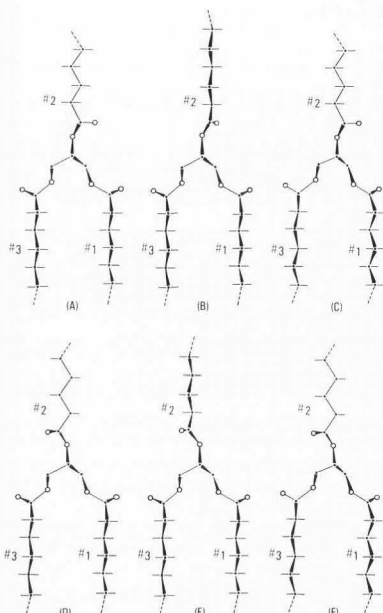


**Fig. 2.** Triglyceride  $\alpha$ -form structures. Tapered bands indicate atoms above or below figure plane, i.e., wide portions above and narrow portions below. Non-tapered bands indicate atoms in plane of figure. Here and in subsequent figures, unless indicated otherwise, carbon atoms are solid circles; oxygen, open circles. Chains are numbered according to convention (Lutton, 1971).

#### Interaction Energy

Molecular interaction energies were derived by summing attractions or repulsions between atom pairs, which were calculated by the following expression (Coiro *et al.*, 1973):

$$V_{(\text{energy})} = \left[ \frac{[(A \cdot \exp(-BR))/R^D] - C/R^6}{R} \right]$$

Results are expressed as Kcal per atom pair when the interatomic distance is in angstroms. Values for constants A, B, C and D depend on the type of interaction; i.e., H...H, C...H, etc. The first part of this expression is the repulsive term; the second part, the attractive term. A greater negative energy value, therefore, represents a better fit between molecules.

#### Mid-chain Energy

When H...H, H...C, and C...C interactions in

hydrocarbons were calculated for each carbon from the middle of the chain to the methyl group (Hagemann and Rothfus, 1979), values for such interactions were found to change nearer the methyl end group. Methylene carbons in the middle of each chain in a particular arrangement have the same energies since they all have similar surroundings and are beyond a cutoff distance of 6 Å for methyl group interaction. Units of middle-of-chain interaction can thus be added to or subtracted from the basic chain length to extrapolate to longer or shorter chain lengths.

End group influence on molecular interaction is differentiated from that of the middle-of-chain by calculating the ratio, middle-of-chain interaction/total interaction. This ratio reflects a diminishing effect of the methyl gap region with increasing chain length. The ratio acquires unexpected significance when it approaches 60 percent for a specific arrangement of molecules. For example, as chain length increases, the ratio is near 60 percent at C22 where the  $\alpha$ -form becomes stable for even-numbered hydrocarbons. Similarly, the ratio is near 60 percent for  $\beta$  monoclinic forms at C26, where a change occurs from  $\beta$  triclinic to  $\beta$  monoclinic subcell arrangement. Furthermore, when the ratio is set at unity in an equation that relates chain length to melting point for  $\beta$  monoclinic forms (Hagemann and Rothfus, 1979), the melting point of polyethylene is predicted to be about 143 °C, which agrees well with 145 °C predicted by Flory and Vrij (1963). Both values are slightly higher than the 138.5 °C melting point obtained for carefully crystallized linear polyethylene of high molecular weight (Parks *et al.*, 1949).

#### Triglycerides

Building molecules in computers is straight forward if atomic coordinates are known from crystallographic studies. Unfortunately, in the case of triglycerides, such data are available only for the  $\beta$ -form (Larsson, 1965a, Gibon *et al.*, 1984). Alternatively, models can be built atom by atom knowing the type of bond, bond length and angle. Commercial software now simplifies such constructions. This work utilized ChemX, developed and distributed by Chemical Design Ltd., Oxford, England.

#### Single Molecules

Figure 2 illustrates abbreviated forms for six of eight  $\alpha$ -form triarachidin molecules built atom by atom for initial studies (Hagemann and Rothfus, 1983b). In Fig. 2, C1-C20 is chain 1, C21-C40 is chain 2, and C41-C60 is chain 3, in keeping with Larsson (1965a). Molecule A has the zigzag plane of chain 2 approximately perpendicular or non-parallel to the zigzag planes of chains 1 and 3. The zigzag planes of chains in molecule B are all approximately parallel. Molecule C is similar to molecule A, except that the zigzag patterns in chains 1 and 3 are opposite; i.e., carbon atoms beneath the plane of the figure in chain 3 are above the plane of the figure in chain 1. A fourth structure, not shown, was similar to B, but with opposite zigzag patterns in chains

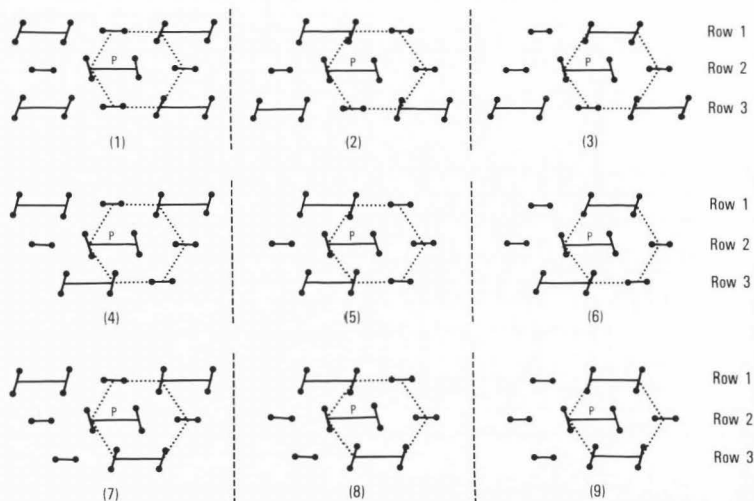


Fig. 3. Possible triglyceride arrangements in hexagonal subcells. One zigzag period is shown for each hydrocarbon chain. Connected zigzag periods represent chains 1 and 3 in upright molecules; individual zigzag periods represent chain 2 in separate inverted molecules. Hydrogen atoms are not indicated.

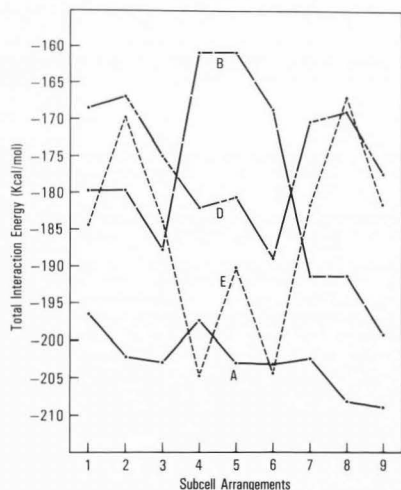


Fig. 4 (at left). Total interaction energy versus subcell arrangement for synchronous oscillation. See Fig. 2 for structure identification.

1 and 3, as in molecule C. When these four molecules are viewed with the glycerol  $\beta$ -hydrogen upward, above the plane of the figure, the carbonyl oxygen of chain 2 lies to the right of an imaginary line through the center of chain 2. A similar set of four molecules can also be made with the carbonyl oxygen of chain 2 on the left side of this center line. Molecules are, therefore, referred to as having parallel or non-parallel chains, carbonyl right or left, and the same or opposite zigzag.

NMR experiments on  $\alpha$ -form triglycerides (Chapman *et al.*, 1960) revealed rotation about the central axes of the fatty acyl chains. This motion is restricted and likely occurs more as oscillations rather than complete revolutions. Thus, chain oscillation was incorporated into the  $\alpha$ -form models in such a way that carbon displacement from the zigzag midposition was least nearest glycerol and greatest near ends of the chains. The rate of oscillation for each chain could be varied to achieve synchronous or asynchronous oscillation of all chains.

#### Molecular Packing

As shown in Figure 3, nine different hexagonal

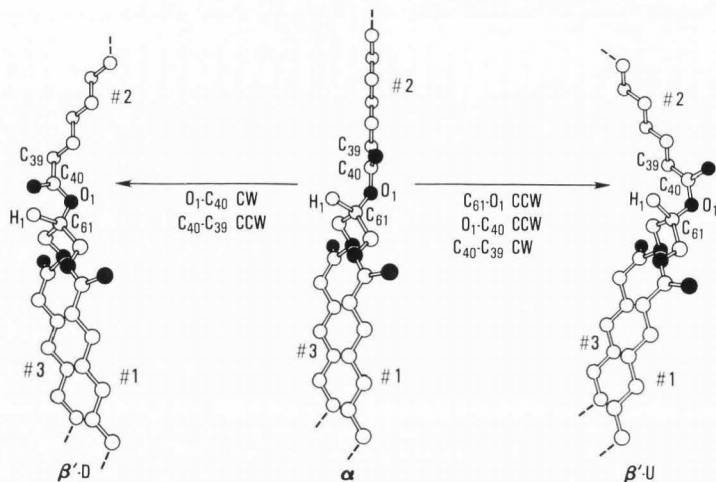


Fig. 5. Triglyceride  $\alpha$  to  $\beta'$ -form transitions by interior bond rotations. Carbon atoms are open circles; oxygen atoms, solid circles; single hydrogen, H1, open circle. CW, clockwise; CCW, counterclockwise.  $\beta'$ -D, methylene chains extend down when molecule is viewed down the H1-C61 bond.  $\beta'$ -U, methylene chains extend upward when molecule is viewed down H1-C61 bond.

subcell packings of triglycerides are possible by alternating upright and inverted molecules with their zigzag chain planes in parallel rows (Hagemann and Rothfus, 1983b). Arrangement 2 in Figure 3 differs from arrangement 1 by a shift of row 1 molecules equivalent to one interchain spacing. Arrangement 3 represents a further interchain spacing shift of row 1. Arrangements 4, 5, and 6 are the same as arrangements 1-3 except that row 3 has undergone one interchain spacing shift. Arrangements 7-9 are derived from arrangements 4-6 by a similar shift of row 3.

Within such arrangements, interaction energies are calculated and compared to search for the best fit between a principal molecule, P, and each of the surrounding molecules. Briefly, a Fortran IV computer program, developed in-house for a Modcomp Classic 32/85 computer (Modular Computer Systems, Fort Lauderdale, FL), determines best fit positions by computing the total interaction energy and then relocating the molecules and recalculating interactions. After the first molecule is built, a predetermined symmetry operation is performed to derive atomic coordinates for atoms of a second molecule, and then atom-atom interaction potentials between the molecules are computed.

A minimization routine (Rosenbrock and Storey, 1966) in our program varies X-, Y-, and Z-axis translation values for the second molecule until a minimum position (maximum stability) is located. The minimum

position is checked by incrementing X, Y, and Z values by 0.1 Å. If these changes produce no lower minimum, the position and values are recorded. If a lower minimum is found, the new coordinates are inserted as starting points and the entire process is repeated.

#### $\alpha$ -forms

The total interaction energy, and consequently the stability, of a solid triglyceride depends on both molecular conformation and subcell arrangement. The extent to which it varies is illustrated in Figure 4 for four molecules: two (A and B) carbonyl right (Fig. 2), and two (D and E) carbonyl left (Fig. 2). Energies are not given for structures having the opposite zigzag pattern in chains 1 and 3. Early results (Hagemann and Rothfus, 1983b) revealed that synchronous oscillation gave slightly greater attractive values. Structure A has non-parallel chains with approximately the same energy content for all arrangements and, therefore, represents the best overall fit. Structure E, with all chains parallel, has relatively stable arrangements, 4 and 6 (Fig. 3), but it also has some that should be among the least stable, 2 and 8 (Fig. 3).

Chain orientation impacts interaction energy only to the extent that it affects the fit of adjacent chains. The orientation of chain 2, either parallel or non-parallel with chains 1 and 3 (Fig. 2), has little effect on total subcell energy. The overall positioning of molecules in the subcell has a greater effect on the total energy than

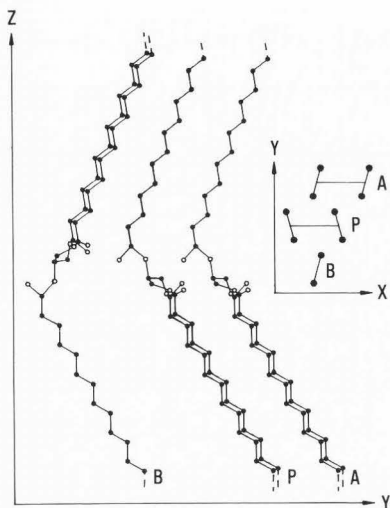


Fig. 6. Asymmetrical chain packing of triglyceride  $\beta'$ -forms. In both views, two molecules (A and B) are packed closely to a principal molecule (P). Hydrogen atoms are not indicated.

does chain orientation (Table I in Hagemann and Rothfus, 1983b). It appears that there is no single preferred combination of structure and arrangement for  $\alpha$ -forms. They probably exist as mixtures of arrangements perhaps enriched by several preferred combinations. This would account for  $\alpha$ -form instability, low heats of fusion, broad melting characteristics, and inability to form single crystals.

#### $\beta'$ -Form

When  $\alpha$ -form triglycerides are heated, they melt and recrystallize into  $\beta'$ -forms and, eventually,  $\beta$ -forms. This process is accompanied by changes in crystal dimensions and, often, changes in properties of materials in which the triglycerides occur. A  $\beta'$  triarachidin model was next examined to better understand the transformation of  $\alpha$ -forms.

Triglycerides in  $\beta'$ -form exhibit an alternating angle of tilt, but it is still uncertain whether the molecules are bent in the glycerol region (Larsson, 1971) or whether their angle of tilt changes at the methyl gap (Hernqvist and Larsson, 1982). The models discussed here are bent in the glycerol region, as shown in Fig. 5. Two different  $\beta'$ -form conformers that fit recorded long spacings from powder X-ray diffraction can be made from each of the previously discussed  $\alpha$ -forms by rotat-

ing specific bonds in different directions (Hagemann and Rothfus, 1988a). The amplitude of each bond rotation depends on the starting  $\alpha$ -form. Clockwise (CW) rotation about the O1-C40 bond and counterclockwise (CCW) rotation about the C40-C39 bond produces a bent  $\beta'$ -form whose fatty acid chains extend downward when the molecule is viewed down the glycerol H1-C61 bond (Fig. 5,  $\beta'$ -D). Similarly, CCW rotation about the C61-O1 and O1-C40 bonds and CW rotation of the C40-C39 bond produces a bent  $\beta'$ -form whose fatty acid chains extend upward when the molecule is viewed down the H1-C61 bond (Fig. 5,  $\beta'$ -U). As with the starting  $\alpha$ -forms (Hagemann and Rothfus, 1983b), the carbonyl oxygen can be either to the right ( $\beta'$ -D) or to the left ( $\beta'$ -U) of H1 as viewed down the H1-C61 bond, and chains 1 and 3 can exhibit opposite or similar zigzag patterns.

Rotations illustrated in Fig. 5 apply to starting  $\alpha$ -forms that have the C40 carbonyl oxygen to the right of H1. When the C40 carbonyl oxygen is to the left of H1, bond rotations are reversed to make  $\beta'$ -D or  $\beta'$ -U. A total of sixteen  $\beta'$ -forms are possible from the eight possible  $\alpha$ -forms. However, when bond rotations were performed on structures having all zigzag chain planes either approximately parallel or non-parallel, the resulting  $\beta'$ -forms were the same, so only eight different  $\beta'$ -forms need be considered.

Studies of  $\beta'$ -form packing reveal that five of the possible nine subcell arrangements pack asymmetrically, as illustrated in Fig. 6, which shows two different views of a principal molecule, P, packed closely to another upright molecule, A, and an inverted molecule, B. The small X-Y insert view is similar to portions of hexagonal arrangements in Fig. 3 (arrangements 2, 3, 4 and 7). As shown in the Y-Z view, space is essentially equal between all chains of molecules P and A, but for molecule B, chains 1 and 3 are much closer to molecule P than is chain 2. Thus, the five  $\beta'$ -form arrangements with molecular packing represented by P and B in Fig. 6 are not likely  $\beta'$ -form packing arrangements due to uneven spacing between chains.

#### $\alpha$ to $\beta'$ Transition

The tendency of one triglyceride form to convert to another and the path followed during conversion both depend on molecular interactions. To better understand how the sequence of molecular events impacts conversion and changes physical properties, the bond rotations required to convert  $\alpha$ -form triglycerides to  $\beta'$  were divided into a number of steps, and at each step intermolecular energies were calculated for interactions between all atoms of molecular pairs (Hagemann and Rothfus, 1988b), such as between P and each of the six surrounding molecules in Figure 3. Calculations were also performed for interactions with eight different molecules across the methyl gaps at both ends of the central molecule. In this manner, an energy curve for the  $\alpha$  to  $\beta'$  transition could be drawn for each interaction around molecule P, and the individual curves could be summed

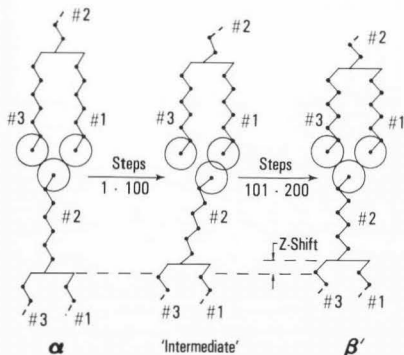


**Fig. 7.** Triglyceride interactions across the methyl gap. Chains are numbered according to convention (Lutton, 1971). Large open circles represent 2 Å Van der Waals radii around methyl groups.

to assess total molecular energy throughout the transition. Insight into crucial features of the transition was then gained by analyzing effects of selective changes on interaction energy.

Several restrictions were placed on molecules and arrangements during the  $\alpha$  to  $\beta'$  transitions described here. All molecules were the symmetrical tuning-fork type, and each row in the subcell arrangement had all zigzag planes parallel. The zigzag planes alternated in successive rows, and the molecules alternated between upright and inverted positions. Chains 1 and 3 in the same molecule were placed in the same row, and the long acyl chains were held rigid during transitions.

#### Methyl Gap Interaction

With triarachidin, intermolecular energy across the methyl gaps amounts to only 3-5 percent of the total interaction energy, but a high repulsive energy region appears in the methyl gap curves. Figure 7 shows three molecular pairs with 2 Å Van der Waals radii around methyl groups. Chain 2 describes an arc during bond rotation, which causes overlap of Van der Waals radii. Overlap also is produced by a programmed shift along the Z-axis. This shift, in keeping with the decrease of X-ray long spacings during  $\alpha$  to  $\beta'$  transitions, is intended to keep methyl groups near 4 Å apart and prevent molecular separation.

When first computed, methyl gap energy for the  $\alpha$  to  $\beta'$  transition of triarachidin indicated a substantial repulsive interaction (ca. 140 Kcal/mol) around step 80 (Fig. 8), as if the transition would not be favored or would not occur unless the molecular packing expanded enough to reduce methyl group overlap. Interestingly, when the Z-axis shift was expressed as an exponential function, which in effect delays the Z-shift until the

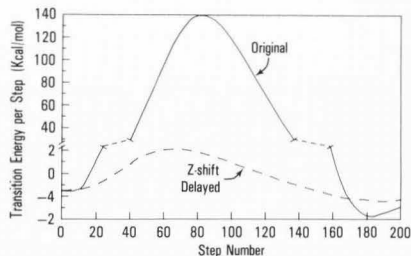


**Fig. 8.** Effect on transition energy of adjustment for methyl gap interaction. Initial  $\alpha$ -form is at Step 0; final  $\beta'$ -form, Step 192. Each step represents 1/200th of total transition parameter shift.

rotated chain begins to return to a vertical position, the repulsive interaction decreased some seventy-fold to ca. 2 Kcal/mol (Fig. 8). Thus, the sequence of molecular events is important, and the transition would be favored in a triglyceride population that could undergo chain rotation and tilt simultaneously. The accompanying change in sample dimension and slightly improved molecular interaction would tend to drive the transition.

#### Side Chain Interaction

In reality, the transition involves more than interaction across the methyl gap. Movement of chain 2 also causes repulsion between adjacent acyl chains. This interference depends on the starting structure, the direction of chain rotation, and the position around molecule P (Fig. 3). Such repulsion was reduced in the triarachidin model by introducing an expansion factor that moved the second molecule away from molecule P near mid-transition. This adjustment, a sine wave function with maximum X-direction expansion near step 100, reduced the repulsive interaction from over 600 Kcal/mol to under 10 Kcal/mol. Energy required to achieve the equivalent of X-direction expansion probably constitutes an additional excitation component in the polymorphic transitions.

#### Transition Energy Profiles

Accumulated transition profiles suggest structure will affect the character of triglyceride form conversion. Figure 9 compares profiles for two different conformers in the same unit cell arrangement.  $\alpha$ -form molecules that start in a carbonyl-left configuration pass through a minimum near step 40. This structure is considered an  $\alpha$ -form since little movement has taken place, and the angle of tilt is about 85 degrees. A minimum at approximately step 160 corresponds to a  $\beta'$ -form that has a long spacing about 1.6 Å longer than the final  $\beta'$ -form at step 200 (49.4 versus 47.8 Å). In contrast, the carbonyl-right  $\alpha$ -form shows no secondary  $\alpha$ -form minimum, but the  $\beta'$  region has a broad minimum, which

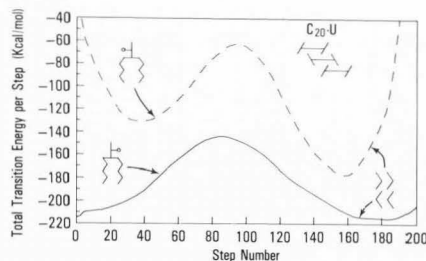


**Fig. 9.** Effect of structure on transition energy. Curves represent sums of interactions between a central subcell molecule and molecules in 14 adjacent positions. Inserts at upper and lower left symbolize triglyceride structures: non-parallel chains, carbonyl left, and opposite zigzag (---); parallel chains, carbonyl right, and same zigzag (—). Insert at upper right indicates subcell arrangement of three upright triarachidin molecules in U configuration (Fig. 4); lower right, methyl gap orientation. Each step represents 1/200th of total transition parameter shift. Initial  $\alpha$ -form is at Step 0; final  $\beta'$ -form, Step 192.

suggests a series of slightly different structures with decreasing long spacings.

For other  $\alpha$ -form conformers, the subcell arrangement affects the energy profile. Results are shown in Fig. 10 for two different subcell arrangements of a non-parallel chain structure with the carbonyl right, an opposite zigzag pattern in chains 1 and 3, and alternating angle of tilt at the methyl gap. Although no secondary  $\alpha$ -form minima are found for either arrangement, the  $\alpha$ -form region is quite flat for nearly 25 steps where the change in angle of tilt would only be a few degrees.

The minimum near step 140 (Fig. 10) represents a long spacing that is greater than any known for  $\beta'$ -forms, which raises question of the existence of additional exploitable triglyceride polymorphs. Similarly, the  $\beta'$  minimum at step 170 corresponds to a long spacing that is 0.9 Å longer than that for the  $\beta'$ -form at step 200. This difference is consistent with the X-ray work of Simpson (Simpson, 1983), who found that long spacings of the two known  $\beta'$ -forms of tristearin differ by about 1 Å.

To summarize, the modeling of  $\alpha$  and  $\beta'$ -forms for even chain length triglycerides and the transition between  $\alpha$  and  $\beta'$  reveals that, among 72 possible  $\beta'$  structure/arrangement combinations, 40 have unsymmetrical molecular spacings, Figure 6, and are therefore unlikely to occur. At least one, as yet unknown,  $\alpha$ -form with an 85 degree angle of tilt is possible; other quite similar and interconvertible  $\alpha$ -forms may also exist. Several  $\beta'$  polymorphs are feasible, which is consistent with the concept that such intermediate forms are

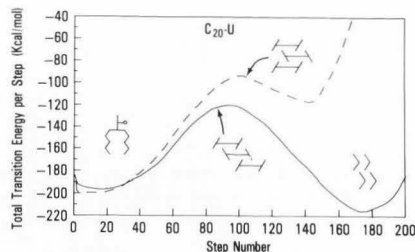


**Fig. 10.** Effect of subcell arrangement on transition energy. Subcells are indicated by three upright molecules. Insert at lower left symbolizes triglyceride structure: non-parallel chains, carbonyl right, and opposite zigzag. Insert at lower right shows methyl gap orientation.  $C_{20}U$  = triarachidin molecule in U configuration (Fig. 4).

important contributors to quality in plastic foods. Unfortunately, modeling predicts that it may be difficult to achieve high concentrations of novel  $\beta'$ -forms because their preparation will probably require control of the starting  $\alpha$ -form, the subcell arrangement, and the way in which aliphatic chains rotate to change conformation. From modeling, the  $\alpha$  to  $\beta'$  transition in a solid fat could occur via a sequence of events that minimizes transition energy; i.e., slight excitation to perturb aliphatic chain association, synchronous chain rotation, chain tilt, and constriction to a more compact configuration.

#### Model Refinement

Evidence that  $\alpha$ -form subcell arrangement affects the type of  $\beta'$  transition product (Figs. 9 and 10) suggests that the quality of triglyceride-rich materials might be regulated by controlling their initial crystallization. Accordingly,  $\alpha$ -form formation from fluid unconstrained molecules remains a potentially fruitful area for modeling research. But the problem entails degrees of molecular freedom and complexities that are better analyzed by different algorithms and supercomputers and/or networked parallel processing.

#### Molecular Perturbations

As discussed in preceding sections, the solid phase transformations of specific  $\alpha$ -forms can be projected by a constrained space-filling model for triglycerides. As expected, this model can help identify potentially useful molecular configurations and problems to be overcome in achieving them. Its ability to resolve similar configurations and distinguish crucial precursors through which useful triglyceride forms can be derived could be improved if there were precise rationales for selecting triglyceride conformations. In the absence of such knowledge, the model has been supplemented with additional degrees of freedom in ways justified by real

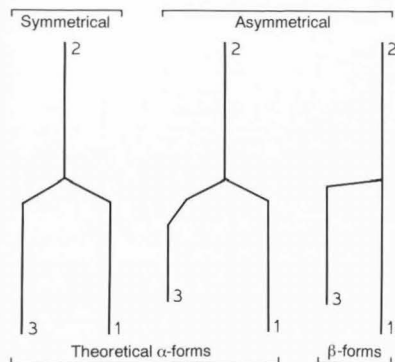


Fig. 11. Variations in triglyceride symmetry. Hydrocarbon chains are indicated by straight lines, and chains are number according to convention (Lutton, 1971).

data and/or experimental hypothesis. Vertical rotational freedom, for example, was incorporated, because NMR studies (Chapman *et al.*, 1960) have shown that triglycerides exhibit rotational freedom in the  $\alpha$ -form. A second vertical motion was incorporated, for purely hypothetical reasons, to accommodate acyl chain vibrations in the directions of their long axes. As with chain rotation, the dislocation from this vibration was greatest at the methyl end group ( $\pm 0.6$  Å) and zero at each carbonyl carbon.

#### Triglyceride Symmetry

In our original model,  $\alpha$ -form molecules were all symmetrical (Hagemann and Rothfus, 1983b) with the methyl groups of chains 1 and 3 in the same plane (Fig. 11, left). This is in contrast to the unsymmetrical or chair type conformation of the  $\beta$ -form (Larsson, 1965a, Gibon *et al.*, 1984), in which chain 3 has side chain character and, with the molecule vertical, methyls on chains 1 and 3 are not in the same plane. That the  $\alpha$ -form structure has an unsymmetrical conformation similar to that of the  $\beta$ -form has been suggested (Hernqvist and Larsson, 1982), but  $^{13}\text{C}$ -NMR studies on  $\alpha$ - and  $\beta$ -tripalmitin (Bociek *et al.*, 1985) and other saturated and unsaturated triglycerides (Gibon *et al.*, 1990) show identical chemical shifts for carbonyl and glycerol carbons on chains 1 and 3. This issue of triglyceride asymmetry was examined by use of a molecule that contained aspects of both types of molecules, symmetrical around chain 1 and asymmetrical around chain 3 (Fig. 11, center).

#### Subcell Minimization

Greater resolution of similar  $\alpha$ -form conformations and better definition of the unit cell arrangements in which symmetric or unsymmetric  $\alpha$ -form molecules

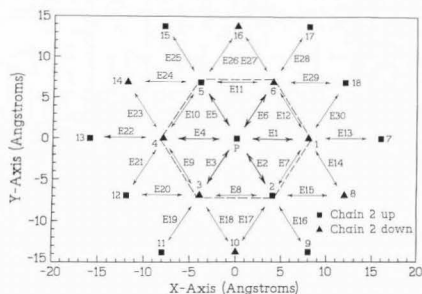
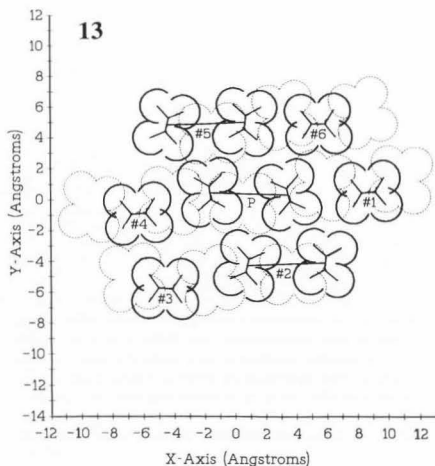


Fig. 12. Schematic for calculation of interaction energy between triglyceride molecules. Basic hexagonal subcell of 7 molecules is outlined with a dashed line. Upright triglycerides (chains 1 and 3 down, chain 2 up) are denoted by solid squares; inverted triglycerides (chain 2 down, chains 1 and 3 up), by solid triangles. Bidirectional lines are energy vectors between molecular pairs.

can exist was sought by a program that minimized interaction energies for a molecular population including P and the seven molecules surrounding it (Fig. 3). The manner of calculation for an entire subcell is illustrated in Fig. 12. Each of the six molecules around P has X, Y, and Z axis freedom as well as vertical rotation; i.e., each has translational, rotational, vibrational and oscillatory motions as described in foregoing sections. A total of 24 parameters are minimized.

Energy calculations are performed between molecule P and each of the surrounding six molecules as indicated by vectors E1 through E6. The E1 through E6 energies are summed to obtain the total interaction energy around P. Similar total interaction energies are then computed for molecules 1 through 6, and the average of the total energies for the seven basic molecules is considered the energy for the subcell packing. Wherever possible, advantage is taken of identities to shorten computation times and reduce the number of molecules. For example, the energy between molecules 1 and 7, E13, can be represented by the interaction between molecules 4 and P, E4. To perform this operation without actually building molecule 7, molecule 4 is temporarily given the Y- and Z-axis translation and vertical rotation values of molecule 1. Likewise, E14 is equivalent to E9 and E30 to E10. Vector E13, however, is not equivalent to E1 as the "faces" between molecules P and 1 are not the same as between 1 and 7 and/or 4 and P. The glycerol region of a triglyceride, being asymmetrical, is not the same on the +X-axis side of molecule P as on the -X-axis side. The same is true for the  $\pm Y$ -directions. E14 is not equivalent to E12, nor is E30 equivalent to E3, since the directions of carbon zigzag planes alternate in successive rows and are approximately perpendicular.



**Fig. 13 (above).** Computer-generated subcell for minimized symmetrical  $\alpha$ -form triglycerides with carbonyl left, non-parallel chains, and same zigzag in chains 1 and 3. Partial circles around zigzag planes represent hydrogen Van der Waals radii for downward acyl chains (dark solid lines) and upward acyl chains (light dashed lines). Connected zigzag planes represent acyl chains of a single molecule.

**Fig. 14 (top right).** Energy curves for minimization of symmetrical  $\alpha$ -form subcell by Zero Edge Crystal Technique. Molecules have carbonyl left, non-parallel chains, and same zigzag in chains 1 and 3.

**Fig. 15 (middle right).** Computer-generated diagram of expanded subcell for symmetrical  $\alpha$ -form triglycerides. See Fig. 13 for description of molecules.

Any one parameter change for each of molecules 1 through 6, therefore, affects the six energy values around the changed molecule. The new energy value obtained for any one molecule is averaged with the total value for each of the other six molecules. If the average energy obtained for the entire subcell is not a better fit than the previous best average minimum, even though the individual molecule may appear favorable, the changed parameter is returned to its original value. The program stores the previous best energy value for each parameter of each molecule P and 1 through 6 as well as the best total minimum value. Generally, computation is terminated when the changes in energy and position over several calculation cycles of all 24 parameters become very small. By this procedure, which we term

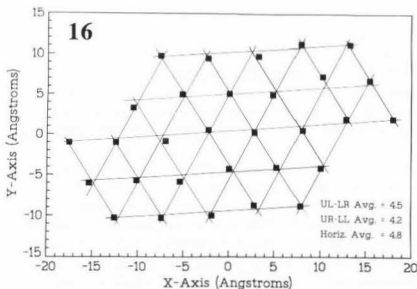
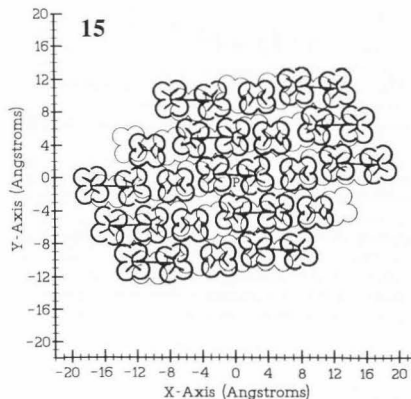
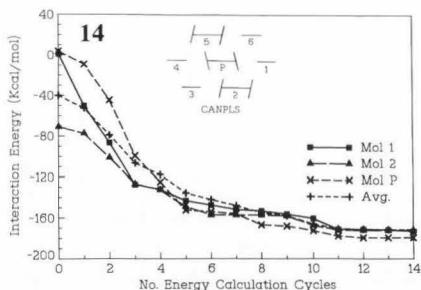


**Fig. 16.** Spacings between centers of zigzag chains in expanded subcell for symmetrical  $\alpha$ -form triglycerides. Molecules positioned as in Fig. 15. Relative position of centers for spacing measurements: UL = upper left; LR = lower right; UR = upper right; LL = lower left.

the Zero Edge Crystal Technique, each molecule is essentially surrounded so that large rotations do not occur and edge effects are virtually eliminated.

#### Symmetric $\alpha$ -form Minimization

Figure 13 shows a minimized arrangement for symmetrical  $\alpha$ -form molecules with non-parallel chains, the carbonyl of chain 2 facing left and the same zigzag pattern in chains 1 and 3 (Fig. 2D). Molecules P, 2, and 5 are upright; 1, 3, 4, and 6 are inverted. To start minimization, the centers of molecules; i.e., the midpoints between connected chains of upright molecules or the midpoints between carbons in the single chains of inverted molecules, are placed 7 Å apart in  $\pm X$ -directions and 6.5 Å apart in the  $\pm Y$ -direction. Carbon atoms 1, 41 (in molecules P, 2 and 5), and 21 (molecules 1, 3, 4, and 6) all start in the same plane.

As computation proceeds, the interaction energy associated with each molecule can be plotted to follow minimization progress. Figure 14 gives results for molecules 1, 2, P and the average of all seven molecules in the subcell shown in Fig. 13. At the tenth cycle, each of the 24 molecular parameters varied during the minimization has been changed ten times. As the curves show for this case, the system very quickly assumes a minimum configuration. Changes become very small after about the sixth cycle. Often the interaction energy for a particular molecule will decrease rapidly and then remain static throughout several cycles. This characteristic, which is exemplified by molecule 2 in Fig. 14, reflects the interrelationships between molecules and suggests a step-like nearest-neighbor dependency during adjustments in molecular packing; perhaps a certain cooperativity or synchrony in molecular motion.

The final positions of the molecules, in this particular case (Fig. 13), are not much different from their initial positions. The molecules merely move closer together with some rotation and/or minor dislocation above or below the initial end-group plane. Molecule 6, for example, rotated 3.8 degrees, and 1 and 4 also rotated 3.0 degrees. Symmetrical movement along the Z-axis was apparent in molecules 1 and 4 (-1 Å) and 2 and 5 (-0.05 Å). Molecules 3 and 6 were somewhat different; they shifted -0.4 and -1.2 Å respectively.

Figure 15 presents an expanded view of this particular case of  $\alpha$ -form packing derived by the minimization procedure. A plot of spacings between zigzag chain centers, Fig. 16, shows that interchain spacing is close, but not identical, to the 4.1 Å spacing that Larsson found for  $\alpha$ -forms by X-ray analysis (Larsson, 1965b). Interestingly, the chains do pack in a slightly distorted hexagonal pattern. Not all theoretical symmetrical  $\alpha$ -forms produce subcell arrangements that are as tightly packed, but most do exhibit this distorted hexagonal arrangement. These results tend to support speculation that liquid triglycerides (or at least those in near-crystal liquids) rotate about a central axis which results in hexagonal symmetry, and that the observed  $\alpha$ -form symmetry arises upon coalescence of the liquid.

#### Asymmetric $\alpha$ -form Minimization

Packing results for an asymmetric  $\alpha$ -form (Fig. 17) molecule, in which chain 3 has side-chain character (Fig. 11), show much less order than those for the symmetrical  $\alpha$ -form (Fig. 13). Molecules P, 1, 2, and 3 pack closely, but the other three molecules are removed from P. Even though the arrangement is more open than that for the symmetrical  $\alpha$ -form, the largest angle of rotation was 1.9 degrees for molecule 1. Z-axis shifts were positive for five molecules (all +0.4 Å), but negative (-0.8 Å) for molecule 3.

An expanded plot of results for the asymmetric  $\alpha$ -form, Fig. 18, suggests reasons why molecules 4, 5, and 6 are removed from P in this particular minimized arrangement. Molecule 4, for example, packs very closely to the two molecules to its left (-X direction). Dislocation of molecule 4 (Fig. 17) in the +X direction would increase its interaction energy with molecule P, but not enough to compensate for the decrease in energy due to disruption of its association with molecules to its left. Thus, the minimization program detects no net improvement in overall energy, and molecule 4 is retained in position. The same is true for molecules 5 and 6. The net result is an arrangement in which chains 1 and 2 from different molecules tend to cluster while chain 3, with side-chain character, does not pack well.

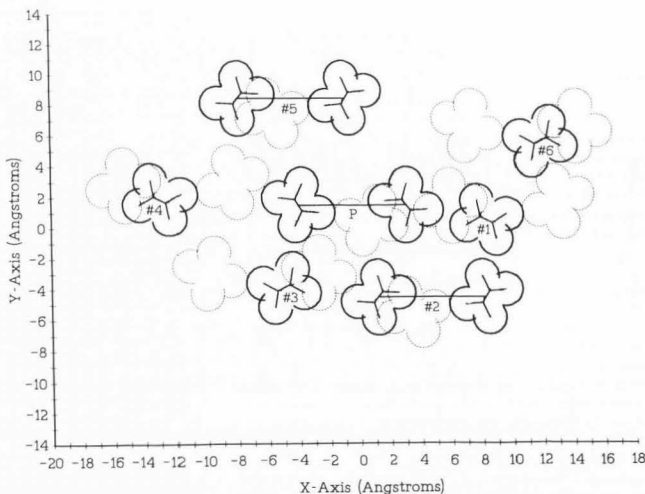
Energy changes that occurred during derivation of the minimized array for the asymmetric  $\alpha$ -form are shown in Fig. 19. The curve for molecule 2, especially illustrates how a particular molecule can be attracted to a small cluster and then remain stationary. The energy associated with molecule 2 did not change after cycle 5 due to its interaction with molecules P, 1, and 3. Other molecules remain static for only one or two cycles, as if the movement of surrounding molecules were prerequisite for further energy gains.

Since structural details are unavailable on  $\alpha$ -form triglycerides, symmetry operations required to build an array like that in Fig. 18 must be developed by experimentation. When molecular packing is not well ordered, as in the case of the asymmetric  $\alpha$ -form, the placement of peripheral molecules may affect configurations at minimum energy. In Fig. 18, two molecules to the left of molecule 4 overlap. The positions of these two molecules are based on relationships between molecules P and 1, and between 5 and 6. Yet overlap occurs. The reason for this packing discrepancy is not yet clear. Perhaps too few molecules were considered, or perhaps a change is needed in the order in which parameters are considered during minimization. It is equally possible that such packing disorders reflect reality and represent one of the causes for general  $\alpha$ -form instability.

#### Conclusions

Triglycerides readily form physical associations that generate supramolecular complexes with novel morphology and valuable properties. Such behavior derives as much from statistical and colligative origins as from

Fig. 17. Computer-generated subcell for minimized asymmetric  $\alpha$ -form triglycerides with carbonyl right, non-parallel chains, and same zigzag in chains 1 and 3. Partial circles around zigzag planes represent hydrogen Van der Waals radii for downward acyl chains (dark solid lines) and upward acyl chains (light dashed lines). Connected zigzag planes represent acyl chains of a single molecule.



covalent chemical structure. Thus, desirable qualities in lipid-rich materials are often achieved by empirical means. Prospects for controlling this behavior, however, are quite appealing and not unrealistic. Regulation of chemical mechanisms by which components associate promises new processing options and new food variety. With constraints allowed by knowledge of chemical composition, molecular configuration, and forces that contribute to macrostructure, systematic investigation by computational methods can identify likely combinations of ingredients and mechanisms by which they may be transformed.

As these studies demonstrate, crystal structures and phase transformations characteristic of lipid populations are amenable to computational analyses. Three concepts from the work are as important as specific results. First, uninterrupted methylene segments determine lipid crystal properties. This is affirmed by the change in preferred hydrocarbon crystal structure as mid-chain interaction energy approaches two-thirds of the total molecular interaction energy. Results further suggest quantitative limits to chain segment effects and imply that unsaturation or other means of segment termination can be used predictably to control methylene segment effects and regulate lipid crystal structure. Second, energetic equivalence allows variety among a finite number of solid lipid configurations, but events early in coalescence may determine which forms predominate. Plausible alternative  $\beta'$ -forms can arise from different starting  $\alpha$ -form triglycerides via different bond rotations and subcell arrangements. Results, however, suggest

that arrays of unsymmetric  $\alpha$ -form saturated triglycerides may not be as stable as those of their symmetric counterparts. It is likely that near-crystalline liquid triglycerides already possess  $\alpha$ -form character; i.e., symmetry and rotation about a molecular axis. Thus, products in which asymmetric or other unusual  $\alpha$ -forms predominate may be difficult to achieve unless formed at higher temperatures in the presence of compounds that interfere with normal  $\alpha$ -form packing. Third, concerted molecular motion and kinetically regulated sequences provide favored mechanisms for triglyceride phase transitions. Molecular populations that can undergo synchronous chain rotation and tilt simultaneously should transform easily. Thermodynamic and temporal regulation could thus be especially important in deriving new food formulations.

Modeling also explains dimensional changes that accompany polymorphic transitions and points to the feasibility of yet uncharacterized  $\alpha$ -form triglycerides through which might be derived a greater variety of specific forms thought to impart quality to certain foods. If microscopic analyses at the molecular level can identify useful forms of lipids, modeling can define paths by which they might be derived. Conversely, if modeling identifies new energetically favored forms of lipids, microscopy should describe them.

#### Acknowledgements

The authors thank the NCAUR computer staff, R. O. Butterfield and D. J. Wolf, for valuable assistance and advice during this work.

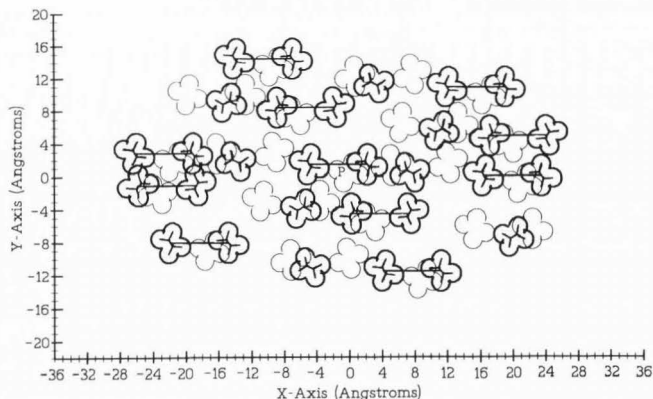


Fig. 18. Computer-generated diagram of expanded subcell for asymmetric  $\alpha$ -form triglycerides. See Fig. 17 for description of molecules.

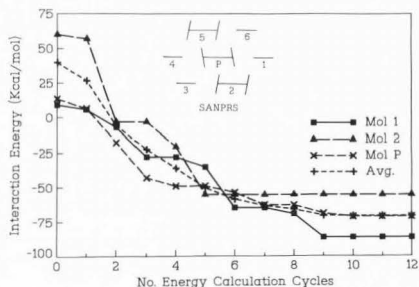


Fig. 19. Energy curves for minimization of asymmetric  $\alpha$ -form subcell by Zero Edge Crystal Technique. Molecules have carbonyl right, non-parallel chains, and same zigzag in chains 1 and 3.

#### References

- Bociek SM, Ablett S, Norton IT. (1985). A  $^{13}\text{C}$ -NMR study of the crystal polymorphism and internal mobilities of the triglycerides, tripalmitin and tristearin. *J. Am. Oil Chem. Soc.* **62**:1261-1266.
- Chapman D, Richards RE, Yorke RW. (1960). Nuclear resonance spectra of the polymorphic forms of glycerides. *J. Chem. Soc.* 436-444.
- Clarkson CE, Malkin T. (1934). Alternation in long-chain compounds. Part II. An X-ray and thermal investigation of the triglycerides. *J. Chem. Soc.* 666-671.
- Coiro VM, Giglio E, Lucano A, Puliti R. (1973). Determination of the molecular packing in the crystal of  $5\alpha$ -androstan-3,17-dione by means of potential energy calculations. *Acta Crystallogr.* **B29**:1404-1409.
- de Jong S, van Soest TC. (1978). Crystal structures and melting points of saturated triglycerides in the  $\beta$ -2 phase. *Acta Crystallogr.* **B34**:1570-1583.
- Flory PJ, Vrij A. (1963). Melting points of linear-chain homologs. The normal paraffin hydrocarbons. *J. Am. Chem. Soc.* **85**:3548-3553.
- Gibon V, Blanpain P, Norberg B, Durant F. (1984). New data about molecular structure of  $\beta$ -trilaurin. *Bull. Soc. Chim. Belg.* **93**:27-34.
- Gibon V, Culot C, Durant F. (1990). Molecular packing of triglycerides studied by solid state NMR spectroscopy. *INFORM.* **1**:355, Abstract VV2.
- Govil G, Hosur RV, Saran A. (1978). Conformational structure of glycerol trivalerate and its relation to phospholipids: studies by NMR and potential energy calculations. *Chem. Phys. Lipids.* **21**:77-96.
- Hagemann JW, Tallent WH, Kolb KE. (1972). Differential scanning calorimetry of single acid triglycerides: effect of chain length and unsaturation. *J. Am. Oil Chem. Soc.* **49**:118-123.
- Hagemann JW, Rothfus JA. (1979). Computer modeling for stabilities and structural relationships of n-hydrocarbons. *J. Am. Oil Chem. Soc.* **56**:1008-1013.
- Hagemann JW, Rothfus JA (1983a). Polymorphism and transformation energetics of saturated monoacid triglycerides from differential scanning calorimetry and theoretical modeling. *J. Am. Oil Chem. Soc.* **60**:1123-1131.
- Hagemann JW, Rothfus JA. (1983b). Computer modeling of theoretical structures of monoacid triglyceride  $\alpha$ -forms in various subcell arrangements. *J. Am. Oil Chem. Soc.* **60**:1308-1314.
- Hagemann JW, Rothfus JA. (1988a). Effects of

chain length, conformation and  $\alpha$ -form packing arrangement on theoretical monoacid triglyceride  $\beta'$ -forms. *J. Am. Oil Chem. Soc.* **65**:638-646.

Hagemann JW, Rothfus JA. (1988b). Computer modeling of  $\alpha$ - to  $\beta'$ -form phase transitions using theoretical triglyceride structures. *J. Am. Oil Chem. Soc.* **65**:1493-1501.

Hernqvist L, Larsson K. (1982). On the crystal structure of the  $\beta'$ -form of triglycerides and structural changes at the phase transitions liq.  $\rightarrow$   $\alpha$   $\rightarrow$   $\beta'$   $\rightarrow$   $\beta$ . *Fette Seifen Anstrichm.* **84**:349-354.

Hosur RV, Saran A, Govil G. (1979). Molecular orbital studies on lipids: conformation of glycerol tri-*valerate* by the PCILO method. *Indian J. Biochem. Biophys.* **16**:165-168.

Kollman P. (1987). Molecular Modeling. *Ann. Rev. Phys. Chem.* **38**:303-316.

Kreissler M, Lemaire B, Bothorel P. (1983). Theoretical conformational analyses of phospholipids. II. Role of hydration in the gel to liquid crystal transition of phospholipids. *Biochim. Biophys. Acta.* **735**:23-24.

Larsson K. (1965a). The crystal structure of the  $\beta$ -form of trilaurin. *Arkiv Kemi.* **23**:1-15.

Larsson K. (1965b). Solid state behavior of glycerides. *Arkiv Kemi.* **23**:35-56.

Larsson K. (1971). Hydrocarbon chain conformation in fats. *Chemica Scripta.* **1**:21-23.

Lutton ES, Fehl AJ. (1970). The polymorphism of odd and even saturated single acid triglycerides, C8-C22. *Lipids.* **5**:90-99.

Lutton ES. (1971). Postulated scheme for  $\beta$  crystal structures of mixed palmitic-stearic triglycerides. *J. Am. Oil Chem. Soc.* **48**:245-247.

Mattice WL. (1979). Size and asymmetry of spatial distributions for unperturbed triglycerides. *J. Am. Chem. Soc.* **101**:732-736.

McAlister J, Yathindra N, Sundaralingam M. (1973). Potential energy calculations on phospholipids. Preferred conformations with intramolecular stacking and mutually tilted hydrocarbon chain planes. *Biochemistry.* **12**:1189-1195.

Parks GS, Moore GE, Renquist ML, Naylor BF, McClaine LA, Fujii PS, Hutton JA. (1949). Thermal data on organic compounds. XXV. Some heat capacity, entropy and free energy data for nine hydrocarbons of high molecular weight. *J. Am. Chem. Soc.* **71**:3386-3389.

Rosenbrock HH, Storey C. (1966). Computational techniques for chemical engineers, Pergamon Press, 64-68.

Simpson TD. (1983). Solid phases of trimargarin: A comparison to tristearin. *J. Am. Oil Chem. Soc.* **60**:95-97.

Smith DPE, Bryant A, Quate CF, Rabe JP, Gerber Ch, and Swalen JD. (1987). Images of a lipid bilayer at molecular resolution by scanning tunneling microscopy, *Proc. Natl. Acad. Sci. USA.* **84**:969-972.

Turner WR. (1971). Normal alkanes. *Ind. Eng. Chem. Prod. Res. Dev.* **10**:238-260.

Zasadzinski JAN, Schneir J, Gurley VE, and Hansma PK. (1988). Scanning tunneling microscopy of freeze-fracture replicas of biomembranes. *Science.* **239**:1013-1015.

### Discussion with Reviewers

**V. J. Gibon:** Please comment about the orthorhombic subcell of the  $\beta'$ -form; it seems that the concept of hexagonal is used also for the  $\beta'$  packing model?

**Authors:** In this first examination of molecular dynamics during polymorphic transformation, similarities between orthorhombic and hexagonal populations made it convenient to follow changes from the hexagonal  $\alpha$ -form configuration. Further refinement of the model could accommodate  $\beta'$  X-ray data, when it is available. The reverse process, excitation and transformation of orthorhombic triglycerides remains for further modeling.

Patterns that approximate hexagonal subcells are evident in arrays of orthorhombic subcells, and infrared data further suggest that hexagonal and orthorhombic triglycerides are similar. When hexagonal  $\alpha$ -forms are cooled to produce sub- $\alpha$ -forms, they exhibit a  $\text{CH}_2$  rocking mode doublet at 719 and 727  $\text{cm}^{-1}$  that is typical of orthorhombic  $\beta'$ -forms (Chapman, 1960, *J. Am. Oil Chem. Soc.*, **37**:73-77). Thus, we think of the hexagonal subcell as a somewhat excited orthorhombic subcell and an appropriate configuration from which to begin transformations into more stable forms.

**K. Larsson:** A characteristic feature of liquid hydrocarbon chains known from liquid-crystals is the lack of crystalline direction due to a high degree of *gauche*-conformation. How do you visualize the " $\alpha$ -form character" in liquid triglycerides?

**Authors:** A certain level of *gauche*-conformation would also be expected in liquid triglycerides due to similarities between hydrocarbons and fatty acid chains. As you have suggested (Larsson, 1972, *Fette Seifen Anstrichm.*, **74**:136-142), sufficient out-of-plane perturbation could easily melt triglycerides, but melting need not destroy all intramolecular order. Indeed, essentially unchanged  $^{13}\text{C}$ -NMR shifts for carbonyl and glycerol carbons in liquid and crystalline  $\alpha$ -form samples (Gibon *et al.*, 1990) suggest little change in polar regions of the molecule upon melting. Portions of the methylene chains held in proximity by covalent bonds to glycerol may continue to interact non-covalently in much the same manner on either side of the melting point. Additional excitation at temperatures further above the melting point would further reduce order around glycerol. Similar logic suggests that stable interactions reestablish easily near glycerol upon cooling a melt. Certainly, the quick formation of  $\alpha$ -form solids in quenched melts suggests some such facilitation. Evidence (Bociek *et al.*, 1985) indicates that the  $\alpha$ -positions of glycerol in single-acid triglycerides are equivalent during coalescence. This equivalence and initial chain associations could be the essential elements of  $\alpha$ -form character, but

the extent to which methylene interaction in molten  $\beta$ -forms, for example, must be disrupted to achieve these features remains unknown. In this regard, it will be interesting to model conformations and interactions in the glycerol region, and to conduct similar studies with mixed-acid and saturated-unsaturated triglycerides.

**V. J. Gibon:** The authors do reference to long spacing values of the  $\alpha$  and  $\beta'$  forms. What about the short spacings for the  $\beta'$  modeling?

**Authors:** True, this work does emphasize X-ray long spacings to the exclusion of short spacings. The emphasis is intentional because long spacings reflect the most dramatic dimensional change and, presumably, the most significant molecular alteration that occurs during polymorphic transition. The current model can be adjusted to fit accepted short spacings without major change in the concept of molecular configuration and motion. With the basic groundwork and modeling techniques in place, future computational experiments exploring alternative transition pathways may lead directly to accurate short spacings without further adjustments.

**K. Sato:** How do you think the present computer modeling is useful to explain the experimental facts that stability of  $\beta'$  is much influenced by differences in chain lengths of saturated-acid triacylglycerols ( $C_n-C_m-C_n$ ;  $n$  and  $m$  are numbers of carbon atoms)? For example,  $C_{16}C_{15}C_{16}$  directly converts from  $\alpha$  to  $\beta$ , but  $C_{16}C_{17}C_{16}$  converts from  $\alpha$  to  $\beta'$ . Do you think this contrast is due to instability in the methyl gap interaction, which is however evaluated less than 5 percent of a total interaction energy in your calculation on  $C_{20}C_{20}C_{20}$ ?

**Authors:** It should be emphasized that the 5 percent contribution of methyl gap energy to total interaction energy was computed for a static crystal structure. Modeling shows that the tendency of a particular triglyceride to occupy any one crystal form,  $\alpha$ ,  $\beta'$  or  $\beta$ , depends as much on kinetic factors and barriers to its transformation as on total interaction energy, which reflects its relative stability. For example, it appears that  $\alpha$ -form saturated single acid triglycerides from acids longer than  $C_{24}$  melt without forming  $\beta'$ - or  $\beta$ -forms because the energy needed to excite the  $\alpha$ -form exceeds that which would be required to melt any  $\beta'$ - or  $\beta$ -forms (Hagemann and Rothfus, 1983a). Even excited molecules that can collapse into more stable configurations may do so via different paths depending upon spatial and temporal conditions. The modeling emphasizes the importance of timing in transverse specific sequences of events to achieve polymorphic transformations. Your mixed triglycerides, which present quite different structures at the methyl gap, may likewise encounter quite different transformation environments. In your  $C_{16}C_{17}C_{16}$ , the  $C_{17}$  chain would penetrate deeper into methyl gap space whereas the  $C_{15}$  methyl in  $C_{16}C_{15}C_{16}$  would not. Likely, increased repulsion of the  $C_{17}$  methyl group will prevent transition to  $\beta$ . In contrast, the shorter chain  $C_{15}$  methyl group may result in voids at the methyl gap but no high energy barriers to a  $\beta$  transition.